PKA phosphorylation couples hepatic inositol-requiring enzyme 1α to glucagon signaling in glucose metabolism

Ting Mao[a,1], Mengle Shao[a,1], Yifu Qiu[a,2], Jialiang Huang[b,c], Yongliang Zhang[a], Bo Song[a], Qiong Wang[a,3], Lei Jiang[a,3], Yi Liu[a], Jing-Dong J. Han[b,c], Pengrong Cao[d], Jia Li[d], Xiang Gao[e], Liangyou Rui[f], Ling Qi[g], Wenjun Li[a], and Yong Liu[a,4]

[a]Key Laboratory of Nutrition and Metabolism, Institute for Nutritional Sciences and [b]Key Laboratory of Computational Biology, Chinese Academy of Sciences–Max Planck Partner Institute for Computational Biology; Shanghai Institutes for Biological Sciences, Chinese Academy of Sciences, Graduate School of the Chinese Academy of Sciences, Shanghai 200031, China; [c]Institute of Genetics and Developmental Biology, Chinese Academy of Sciences, Beijing 100101, China; [d]National Center for Drug Screening, Shanghai Institute of Materia Medica, Chinese Academy of Sciences, Shanghai 201203, China; [e]Model Animal Research Center, Nanjing University, Nanjing 210093, China; [f]Department of Molecular and Integrative Physiology, University of Michigan Medical School, Ann Arbor, MI 48109; and [g]Division of Nutritional Sciences, Cornell University, Ithaca, NY 14853

Edited by Marc R. Montminy, The Salk Institute for Biological Studies, La Jolla, CA, and approved August 15, 2011 (received for review May 9, 2011)

The endoplasmic reticulum (ER)-resident protein kinase/endoribonuclease inositol-requiring enzyme 1 (IRE1) is activated through transautophosphorylation in response to protein folding overload in the ER lumen and maintains ER homeostasis by triggering a key branch of the unfolded protein response. Here we show that mammalian IRE1α in liver cells is also phosphorylated by a kinase other than itself in response to metabolic stimuli. Glucagon-stimulated protein kinase PKA, which in turn phosphorylated IRE1α at Ser^{724}, a highly conserved site within the kinase activation domain. Blocking Ser^{724} phosphorylation impaired the ability of IRE1α to augment the up-regulation by glucagon signaling of the expression of gluconeogenic genes. Moreover, hepatic IRE1α was highly phosphorylated at Ser^{724} by PKA in mice with obesity, and silencing hepatic IRE1α markedly reduced hyperglycemia and glucose intolerance. Hence, these results suggest that IRE1α integrates signals from both the ER lumen and the cytoplasm in the liver and is coupled to the glucagon signaling in the regulation of glucose metabolism.

endoplasmic reticulum stress | G protein-coupled receptor | metabolic disease

Homeostasis in the endoplasmic reticulum (ER) is central to the proper function and survival of eukaryotic cells. Accumulation of unfolded/misfolded proteins in the ER lumen triggers the unfolded protein response (UPR), which reduces ER stress by enhancing the ER's capacity to manage the workload of protein folding (1). The mammalian UPR is executed through three canonical signaling branches mediated by the ER-localized transmembrane proteins, inositol-requiring enzyme 1 (IRE1), PKR-like endoplasmic reticulum kinase (PERK), and activating transcription factor 6 (ATF6). Conserved from yeast to humans, IRE1 is the most ancient sensor of ER stress and possesses both protein Ser/Thr kinase and endoribonuclease (RNase) activities (1–5). Under ER stress conditions, IRE1 is activated through dimerization and transautophosphorylation (6, 7). Activation of IRE1α results in the nonconventional splicing of X-box binding protein 1 (*Xbp1*) mRNA to generate an active form of this transcription factor that induces a major transcriptional program of the UPR (8–10). Interestingly, chemical manipulation of the activation mode of IRE1α has been shown to generate alternate RNase outputs (11), suggesting complex structural features of this molecule upon autophosphorylation within its kinase domain to activate its RNase activity. Recently reported crystal structures of the cytoplasmic kinase/endoribonuclease region of yeast Ire1, as well as the dephosphorylated human IRE1α, revealed a dimeric orientation (12, 13) or oligomeric arrangements (14) for transautophosphorylation, implying that this kinase is unlikely to be accessible for phosphorylation by other kinases than itself (14) and the XBP1-specific RNase activity is dependent on autophosphorylation (12). However, it remains largely unknown if mechanisms aside from autophosphorylation are operative in activating IRE1, particularly under physiological or pathophysiological conditions.

The ER is thought to be a critical nutrient-sensing organelle that is functionally linked with metabolic responses (15). Emerging evidence has shown that in mammals, the UPR pathways are associated with changes in metabolic cues (15–19), as well as with obesity-associated metabolic stress conditions (20–23). Given our previous finding that glucose stimulation of IRE1α phosphorylation in pancreatic β-cells represents a glucose-sensing event (18), we considered the possibility that induction of IRE1α phosphorylation in response to metabolic stimuli could reflect a general phenomenon of physiological activation of this UPR sensor. Here we show that IRE1α can integrate metabolic signals through phosphorylation by PKA of the G protein-coupled receptor (GPCR) pathway and is coupled to glucose metabolism in liver cells, thereby contributing to disruption of glucose homeostasis under obesity-associated metabolic ER stress.

Results

IRE1α Is Metabolically Activated by Glucagon in the Liver. To test if mammalian IRE1α is able to sense changes in metabolic cues, we first examined the phosphorylation status of liver IRE1α in mice under fasted or fed states. In parallel with elevated phosphorylation of cAMP response element-binding protein (CREB), phosphorylation of IRE1α at Ser^{724}, a highly conserved positive regulatory site (Ser^{841} in yeast Ire1) within its activation segment of the kinase domain (12–14), markedly increased upon fasting as detected by a phospho-site–specific antibody (Fig. 1*A*). In contrast, fasting did not enhance the phosphorylation of eukaryotic translation initiation factor 2α (eIF2α), the downstream target of the PERK pathway of the UPR (1). Furthermore, glucagon, the principal hormone that regulates hepatic glucose production in the fasted state, robustly augmented the phosphorylation of IRE1α but not eIF2α in livers of mice (Fig. 1*B*), as well as in

Author contributions: T.M., M.S., Y.Q., and Yong Liu designed research; T.M., M.S., Y.Q., Y.Z., B.S., Q.W., and L.J. performed research; Yi Liu, P.C., J.L., X.G., and L.Q. contributed new reagents/analytic tools; T.M., M.S., J.H., J.-D.J.H., L.R., L.Q., W.L., and Yong Liu analyzed data; and T.M. and Yong Liu wrote the paper.

The authors declare no conflict of interest.

This article is a PNAS Direct Submission.

Data deposition: The microarray data are to be deposited in the National Center for Biotechnology Information (NCBI) Gene Expression Omnibus (GEO) database, www.ncbi.nlm.nih.gov/geo (accession nos. GSE31638).

[1]T.M. and M.S. contributed equally to this work.

[2]Present address: University of California, San Francisco, CA 94158.

[3]Present address: University of Texas Southwestern Medical Center at Dallas, Dallas, TX 75390.

[4]To whom correspondence should be addressed. E-mail: liuy@sibs.ac.cn.

This article contains supporting information online at www.pnas.org/lookup/suppl/doi:10.1073/pnas.1107394108/-/DCSupplemental.

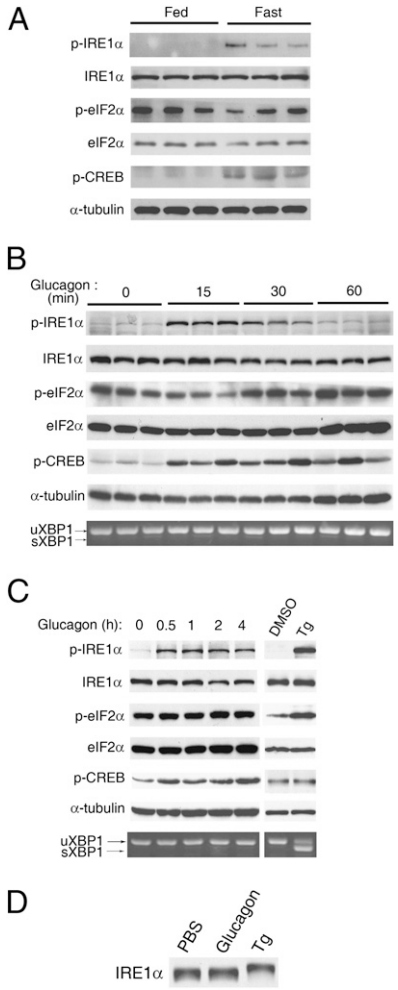

Fig. 1. Glucagon stimulates the phosphorylation of hepatic IRE1α. (*A*) Fasting induced hepatic IRE1α phosphorylation. Male C57BL/6 mice were ad libitum fed or subjected to a 6-h fast. Liver extracts were analyzed by immunoblotting using the indicated antibodies. Results are shown for three individual mice in the fed or fasted state, representative of two independent experiments. (*B* and *C*) Glucagon stimulated IRE1α phosphorylation in vivo and in primary hepatocytes. (*B*) Mice were treated for the indicated time intervals (n = 3 per group) by intraperitoneal injection of glucagon (100 μg/kg body weight). (*C*) Mouse primary hepatocytes were treated with 100 nM glucagon as indicated, or with dimethyl sulfoxide (DMSO) or thapsigargin (Tg, 1 μM) for 1 h. Protein extracts were analyzed by immunoblotting, and spliced (s) and unspliced (u) *Xbp1* mRNA transcripts were measured by RT-PCR. Results are representative of at least three independent experiments. (*D*) Glucagon induced a distinct phosphorylation state of IRE1α from that caused by ER stress. Primary hepatocytes were treated with PBS, 100 nM glucagon, or 1 μM Tg for 1 h. Immunoblotting was performed for band-shift analysis using the IRE1α antibody. Results are representative of three independent experiments.

isolated primary hepatocytes (Fig. 1*C*), suggesting that glucagon selectively affected the IRE1α branch of the UPR pathways. Notably, glucagon-induced IRE1α phosphorylation at Ser^{724} did not increase the splicing of *Xbp1* mRNA (Fig. 1 *B* and *C*), contrasting that observed upon treatment with thapsigargin, a chemical inducer of ER stress (Fig. 1*C*). Although up-regulating the mRNA expression of two gluconeogenic genes, *G6pase* and *Pepck* (*SI Appendix,* Figs. S1*A* and S2*A*), glucagon did not increase the mRNA abundance of two UPR genes, *Chop* and *Bip* (*SI Appendix,* Figs. S1*B* and S2*A*). On the other hand, thapsigargin-induced phosphorylation of IRE1α (Fig. 1*C*) was accompanied by increased mRNA abundance of *Chop* and *Bip* but not that of *G6pase* and *Pepck* (*SI Appendix,* Fig. S2*B*). As an internal control, *actin* mRNA expression was not affected in hepatocytes when exposed to either glucagon or thapsigargin (*SI Appendix,* Fig. S2*C*). These results indicate that glucagon-induced acute phosphorylation of IRE1α represents a metabolic activation event, which is distinct from that induced by typical ER stress. In keeping with this idea, glucagon-stimulated phosphorylation did not cause a detectable shift of the IRE1α protein when examined by immunoblot analysis (Fig. 1*D*), in contrast to the thapsigargin-induced shift that most likely resulted from multiple-site autophosphorylation of IRE1α upon ER stress (13, 14). These data thus raise the possibility that mechanisms aside from transautophosphorylation are operative in initiating the metabolic activation of the IRE1α pathway.

Next, we investigated whether IRE1α acts as a critical component in mediating glucagon's metabolic effects. In comparison with primary liver cells infected with a scrambled control adenovirus (Ad-shCON), knockdown of the expression of IRE1α with Ad-shIRE1α-#1 or -#2, which expressed one of two shRNAs directed against IRE1α, significantly compromised the stimulation by glucagon of the mRNA expression of *G6pase* and *Pepck* without affecting the phosphorylation of CREB (Fig. 2*A*). Moreover, transcriptomic analysis (*SI Appendix,* Fig. S3*A*) revealed a remarkable blunting effect of IRE1α knockdown on glucagon-regulated gene-expression programs in liver cells, as indicated by a Pearson Correlation Coefficient (PCC) of −0.64 (Fig. 2*B*). Among genes that were significantly up-regulated or down-regulated by glucagon induction, ∼37% or ∼43% were oppositely affected by IRE1α knockdown (Fig. 2*B*), which were enriched by ∼9.5- or ∼11.5-fold over all array-probed genes (P < 2.2E-16, Fisher's exact test) (*SI Appendix,* Fig. S3*B*). Parametric analysis of gene set enrichment (PAGE) also showed a profound influence of IRE1α deficiency upon glucagon-regulated cellular pathways and biological processes (*SI Appendix,* Fig. S3*C*), including those associated with carbohydrate, lipid, and amino acid metabolism. Notably, among transcription factors involved in the regulation of lipid metabolism and enzymes related to triglyceride synthesis, which were found to be up-regulated under ER stress in hepatocytes from mice with liver-specific deletion of IRE1α (24), IRE1α knockdown under glucagon-stimulated conditions did not cause prominent changes in the expression of *C/ebpβ*, *C/ebpδ*, or *Pparγ*, but resulted in increased expression of *Scd1*, *Dgat1/2*, and *Acc1* (*SI Appendix,* Fig. S3*D*). Importantly, knockdown of hepatic IRE1α markedly decreased the glucose production capacity (Fig. 2*C*) of hepatocytes isolated from Ad-shIRE1α-#2–infected mice in the absence or presence of stimulation with forskolin, a chemical activator of protein kinase A (PKA) of the glucagon signaling pathway. Suppression of hepatic IRE1α in mice also led to a significant attenuation of the hyperglycemic response to glucagon (Fig. 2*D*). Together, these results demonstrate that the IRE1α pathway of the UPR in the liver is responsive to glucagon stimulation and is functionally implicated in mediating glucagon's regulatory actions in glucose metabolism.

PKA Is Required for Glucagon-Induced Phosphorylation of IRE1α. Glucagon triggers a cascade of signal transduction events through activation of its seven-transmembrane GPCR. Stimulation of adenylate cyclase activity through the stimulatory G protein ($G\alpha_s$) leads to increased cAMP production, thereby activating PKA for CREB phosphorylation (25). Glucagon can also increase the intracellular calcium in a phospholipase C (PLC)-dependent manner (26). To test the idea that a protein kinase other than IRE1α itself may link glucagon receptor signaling with the observed stimulation of IRE1α phosphorylation, we examined whether PKA is involved. Interestingly, pharmacological PKA inhibitor H89, but not PLC inhibitor U73122, blunted glucagon-stimulated phosphorylation of IREα as well as CREB in primary hepatocytes (Fig. 3*A*). In contrast, H89 showed no such inhibitory effect on thapsigargin-induced phosphorylation of IRE1α (*SI Appendix,* Fig. S4*A*). Epinephrine, another agonist of $G\alpha_s$-coupled receptor and regulator of hepatic glucose metabolism, could also stimulate the phosphorylation of

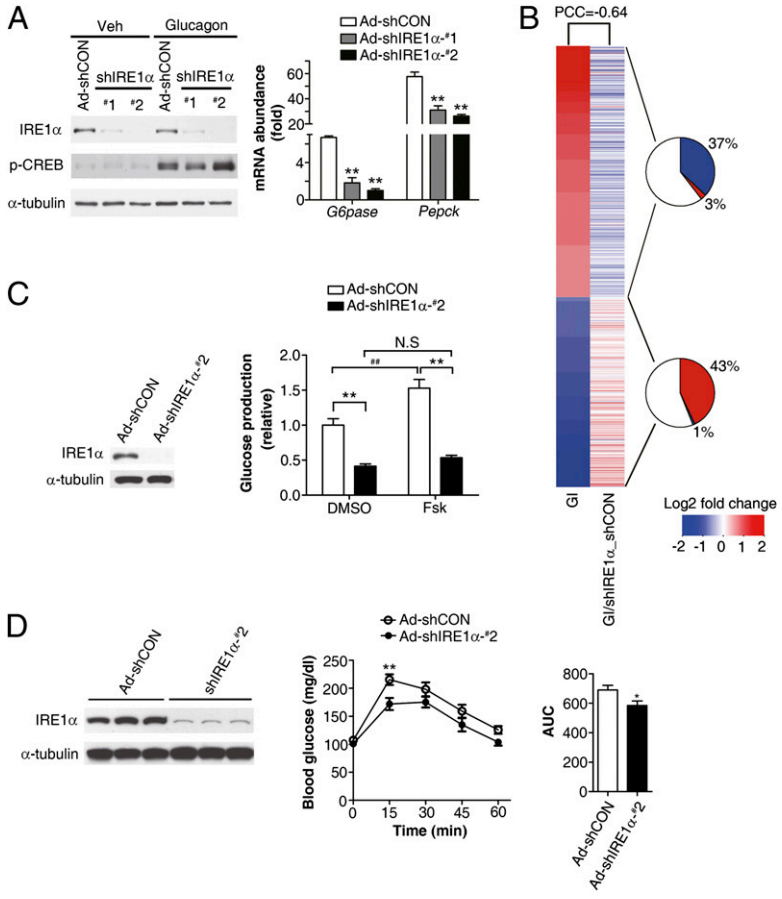

Fig. 2. IRE1α mediates glucagon's metabolic effects in liver cells. (*A*) IRE1α knockdown reduced glucagon-induced expression of gluconeogenic genes. Primary hepatocytes, infected for 72 h with the indicated adenoviruses, were incubated with 100 nM glucagon for 4 h. Immunoblotting was performed for IRE1α expression analysis. Expression of *Pepck* and *G6pase* was analyzed by real-time RT-PCR using *actin* as an internal control, shown as averaged fold-induction by glucagon ± SEM (n = 3 independent experiments). $^{**}P < 0.01$ compared with Ad-CON by one-way ANOVA. (*B*) Impact of IRE1α knockdown on glucagon-induced transcriptomic changes in hepatocytes. Microarray analysis was performed as described in *SI Appendix*, Fig. S3. Heat maps represent averaged fold changes of gene expression from three independent experiments, showing differentially expressed genes caused by glucagon induction (GI) as aligned with changes of these genes as a result of IRE1α knockdown in the presence of glucagon stimulation (GI/shIRE1α_shCON). PCC value was calculated between the fold-changes in the two heat maps. The pie charts indicate the percentages of glucagon-up-regulated or -down-regulated genes that were oppositely changed or unaltered by IRE1α knockdown. (*C* and *D*) IRE1α deficiency reduced glucose production from liver cells and attenuated the hyperglycemic response to glucagon in vivo. Mice were infected with Ad-shCON or Ad-shIRE1α-$^{\#}$2 through tail vein injection. (*C*) Primary hepatocytes were isolated after 5 d of infection and glucose production was measured in the absence or presence of 10 μM forskolin (Fsk). Data are presented as the mean ± SEM (n = 3 independent experiments). $^{**}P < 0.01$, $^{\#\#}P < 0.01$ by two-way ANOVA. (*D*) Glucagon challenge test. Mice infected for 10 d were injected intraperitoneally with glucagon (150 μg/kg) after a 15-h fast. Blood glucose was measured at the indicated time points after glucagon injection. The areas under the curve (AUC) were shown as the mean ± SEM (n = 10–11/group). $^{*}P < 0.05$, $^{**}P < 0.01$ by two-way ANOVA or t test.

IRE1α, which was likewise attenuated by H89 (Fig. 3*B*). Arguing for a direct connection of cAMP-dependent PKA activation with IRE1α phosphorylation, both forskolin (an activator of adenylate cyclase) and Br-cAMP (a cAMP analog) were able to increase the phosphorylation of IRE1α in liver cells (*SI Appendix*, Fig. S4*B*). Ruling out possible nonspecific effects of H89 (27), adenovirus-mediated knockdown of hepatic PKA expression with Ad-shPKA abolished glucagon-stimulated but not thapsigargin-induced phosphorylation of IRE1α (Fig. 3*C*). These results clearly demonstrate that PKA is required for the phosphorylation of IRE1α evoked by the GPCR-cAMP pathway. To verify further that glucagon-induced phosphorylation of IRE1α is independent of its capability of transautophophorylation, we used a Lys^{599}→Ala^{599} (K599A) substitution kinase-dead mutant of human IRE1α that was unable to autophosphorylate spontaneously (18) when adenovirally overexpressed in primary hepatocytes, as analyzed using the phospho-site–specific antibody that could not detect the Ser^{724}→Ala^{724} (S724A) mutant of IRE1α (Fig. 3*D*). Overexpressed S724A mutant failed to be autophosphorylated at this site located within the structurally disordered central activation segment of IRE1α (12), and blocking its phosphorylation may cause disruption of IRE1α's functional outputs (17, 18). Consistently, glucagon increased the phosphorylation at Ser^{724} of IRE1α-K599A, which did not alter its inactivity for splicing *Xbp1* mRNA (Fig. 3*D*). In contrast, thapsigargin was unable to increase overtly the phosphorylation of IRE1α-K599A (*SI Appendix*, Fig. S5*A*) through activation of the endogenous IRE1α. Because the IRE1α-K599A mutant could be transphosphorylated at a detectable level by the overexpressed EGFP-IRE1α-WT fusion protein that was robustly autophosphorylated (*SI Appendix*, Fig. S5*B*), Ser^{724} within the IRE1α-K599A mutant might be more preferably phosphorylated by PKA than by the endogenous IRE1α. In addition, H89 attenuated glucagon-induced phosphorylation of IRE1α-K599A at Ser^{724}, but not that of IRE1α-WT resulting from forced autophosphorylation (Fig. 3*D*). Notably, the S724A mutant retained its ability to splice *Xbp1* mRNA, suggesting that phosphorylation at this single site may not be essential for activating its RNase activity. Given that Ser^{724} is positioned within a consensus target sequence (RHS) of PKA (28), we reasoned that IRE1α may be a direct phosphorylation substrate of PKA. Indeed, purified recombinant PKA (*SI Appendix*, Fig. S6*A*) but not PKCε (*SI Appendix*, Fig. S6*B*) increased the phosphorylation at Ser^{724} of immunoprecipitated Flag-tagged IRE1α-WT or IRE1α-K599A from hepatocytes (Fig. 3*E*), as well as a purified cytoplasmic fragment of IRE1α (Fig. 3*F*), both of which could be inhibited by H89. Thus, these data revealed a previously unanticipated PKA-dependent mechanism by which hepatic IRE1α phosphorylation is metabolically linked to the GPCR pathway.

Blocking Phosphorylation at Ser^{724} Affects the Metabolic Output of IRE1α. We then sought to assess the functional significance of PKA-directed phosphorylation at Ser^{724} of hepatic IRE1α. First, band-shift analysis by immunoblotting showed a considerably less extent of shift of the adenovirally overexpressed IRE1α-S724A mutant protein than that of IRE1α-WT (Fig. 4*A*), whereas glucagon-induced phosphorylation did not cause a detectable shift of the autophosphorylation-deficient mutant IRE1α-K599A (Fig. 4*A*). This finding indicates that blocking Ser^{724} phosphorylation might impede IRE1α from being fully activated through transautophosphorylation. Next, we examined the effects of deficiency in Ser^{724} phosphorylation upon IRE1α-evoked changes of the hepatic transcriptome. Genome-wide transcriptional profiling analysis (*SI Appendix*, Fig. S7*A*) showed that S724A mutation significantly attenuated IRE1α-induced changes of gene-expression profiles, as indicated by a PCC of −0.51 (Fig. 4*B*). For genes significantly up-regulated or down-regulated by IRE1α, ~21% or ~13% were oppositely influenced by S724A mutation (Fig. 4*B*),

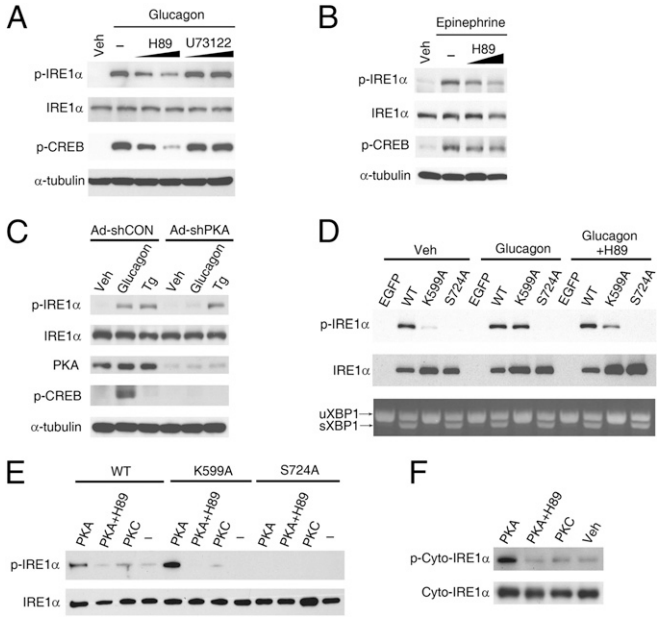

Fig. 3. PKA is directly responsible for phosphorylating IRE1α. (*A* and *B*) Inhibition of PKA decreased glucagon- or epinephrine-induced phosphorylation of IRE1α. (*A*) Primary hepatocytes precultured for 30 min with PKA inhibitor H89 (at 5 and 10 μM) or PLC inhibitor U73122 (at 5 and 15 μM) were treated with 100 nM glucagon or PBS/DMSO (Veh) for 1 h. (*B*) Hepatocytes precultured with 5 and 10 μM H89 were stimulated with 10 μM epinephrine for 10 min. Immunoblotting was performed with the indicated antibodies. (*C*) PKA knockdown blunted glucagon-stimulated IRE1α phosphorylation. Hepatocytes infected for 72 h with adenoviruses Ad-shCON or Ad-shPKA were subsequently incubated for 1 h with 100 nM glucagon or 1 μM Tg. (*D*) Glucagon-induced phosphorylation of IRE1α was independent of its capability of autophosphorylation. Hepatocytes were infected with adenoviruses expressing EGFP, Flag-tagged human wild-type (WT) IRE1α or IRE1α-K599A and IRE1α-S724A mutants. Cells with or without preincubation for 30 min in 10 μM H89 were then treated with 100 nM glucagon for 1 h. Phosphorylation of IRE1α and splicing of *Xbp1* mRNA were analyzed. (*E* and *F*) PKA directly phosphorylated IRE1α in vitro. (*E*) Hepatocytes were infected for 48 h with adenoviruses expressing the indicated forms of Flag-tagged IRE1α. IRE1α proteins were immunoprecipitated with Flag antibody and subsequently incubated with purified mouse PKA or human PKCε at 30 °C for 1 h. (*F*) Purified recombinant protein of the cytoplasmic portion of human IRE1α was likewise incubated with PKA or PKC. Phosphorylation of IRE1α was analyzed by immunoblotting. All results are shown as representative of three (*A*–*E*) or two (*F*) independent experiments.

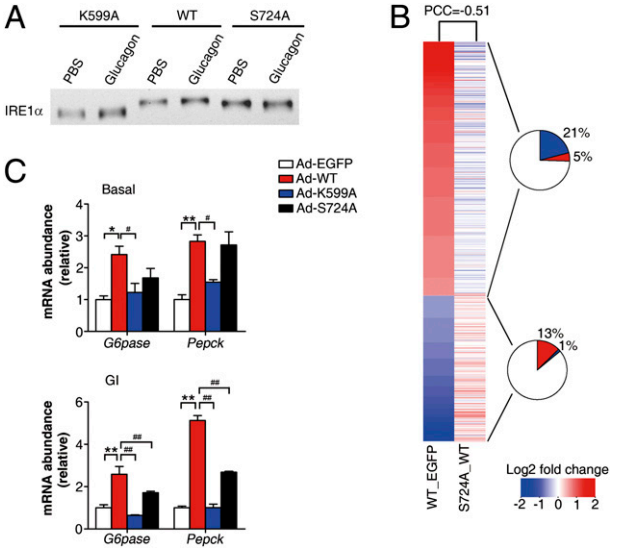

Fig. 4. Phosphorylation at Ser^{724} dictates the functional output of IRE1α. (*A*) Blocking Ser^{724} phosphorylation resulted in altered autophosphorylation status of IRE1α. Primary hepatocytes infected with adenoviruses expressing the indicated forms of Flag-tagged human IRE1α were treated with PBS or 100 nM glucagon for 1 h. Immunoblotting was performed using IRE1α antibody for band-shift analysis. (*B*) Impact of disruption of Ser^{724} phosphorylation on IRE1α-evoked transcriptomic changes in hepatocytes. Microarray analysis was performed as described in *SI Appendix*, Fig. S7. Heat maps represent averaged fold-changes of gene expression from three independent experiments, showing differentially expressed genes upon IRE1α-WT overexpression (WT versus EGFP control) as aligned with changes of these genes caused by S724A mutation (S724A versus WT). PCC value was calculated, and the pie charts indicate the percentages of IRE1α up-regulated or down-regulated genes, which were oppositely changed or unaltered by S724A mutation. (*C*) S724A mutation impaired IRE1α-WT up-regulation of gluconeogenic genes. Hepatocytes infected with the indicated adenoviruses were treated with PBS or 100 nM glucagon for 1 h. The mRNA abundance of *Pepck* and *G6pase* was determined by real-time RT-PCR using *actin* as an internal control. Data are shown as the mean ± SEM after normalization to the Ad-EGFP control. **P* or $^{\#}P < 0.05$, ***P* or $^{\#\#}P < 0.01$ by one-way ANOVA.

which were enriched by ~5.3- or ~9.0-fold, respectively, relative to all genes ($P < 2.2E-16$, Fisher's exact test) (*SI Appendix*, Fig. S7*B*). PAGE analysis also revealed a large impact of S724A mutation upon IRE1α-elicited alterations in metabolism-related cellular pathways (*SI Appendix*, Fig. S7*C*), including gluconeogenesis. Next, we verified the importance of Ser^{724} phosphorylation in IRE1α regulation of gluconeogenic genes by quantitative RT-PCR. Under glucagon-stimulated conditions, S724A mutation significantly blunted—and K599A mutation completely abolished—the ability of IRE1α to augment the mRNA abundance of *G6pase* and *Pepck* (Fig. 4*C*). These data suggest that phosphorylation of hepatic IRE1α at Ser^{724}, which is also targeted by PKA, dictates the functional output of IRE1α, and may constitute a key step in glucagon regulation of the gluconeogenic program. As genetic ablation of hepatic IRE1α or XBP1 has been shown to affect lipid metabolism (24, 29, 30), we wondered whether XBP1 can mediate IRE1α's effect on the up-regulation of gluconeogenic genes. Surprisingly, adenoviral overexpression in hepatocytes of the spliced form of XBP1 (*SI Appendix*, Fig. S8*A*) did not enhance, but rather suppressed, the expression of *G6pase* and *Pepck* upon glucagon stimulation (*SI Appendix*, Fig. S8*B*), and markedly increased the expression of *Bip*. This finding is consistent with a recent study documenting that modest hepatic overexpression of the spliced form of XBP1 protein in mouse models suppressed the gluconeogenic program and improved glucose metabolism (31). Moreover, adenovirus-mediated knockdown of XBP1 expression in hepatocytes (*SI Appendix*, Fig. S8*C*) significantly reduced the expression of the XBP1 target gene *Erdj4* upon ER stress, but did not affect glucagon-induced expression of *G6pase* and *Pepck* (*SI Appendix*, Fig. S8*D*). Consistent with the reported findings that sXBP1 levels were increased in a pancreatic β-cell line upon prolonged exposure (14 h) to forskolin (32), chronic treatment of hepatocytes with glucagon for 16 h also increased *Xbp1* mRNA splicing (*SI Appendix*, Fig. S9*A*), without further influencing the expression of *G6pase* and *Pepck* (*SI Appendix*, Fig. S9*B*). These results thus argue for a lesser role for sXBP1 in glucagon up-regulation of gluconeogenic genes, further suggesting that IRE1α most likely contributes, in an XBP1-independent manner, to glucagon-elicited metabolic regulatory programs in the liver.

Highly Phosphorylated Hepatic IRE1α Is a Hyperglycemic Driver Under Metabolic ER Stress. To gain insights into the physiological significance of PKA-mediated crosstalk between IRE1α and the glucagon signaling pathway, we determined the phosphorylation status of hepatic IRE1α from leptin receptor-deficient *db*/*db* mice (18), which displayed hyperglycemia and hyperglucagonemia in the fasted state (*SI Appendix*, Fig. S10*A*). In comparison with wild-

CELL BIOLOGY

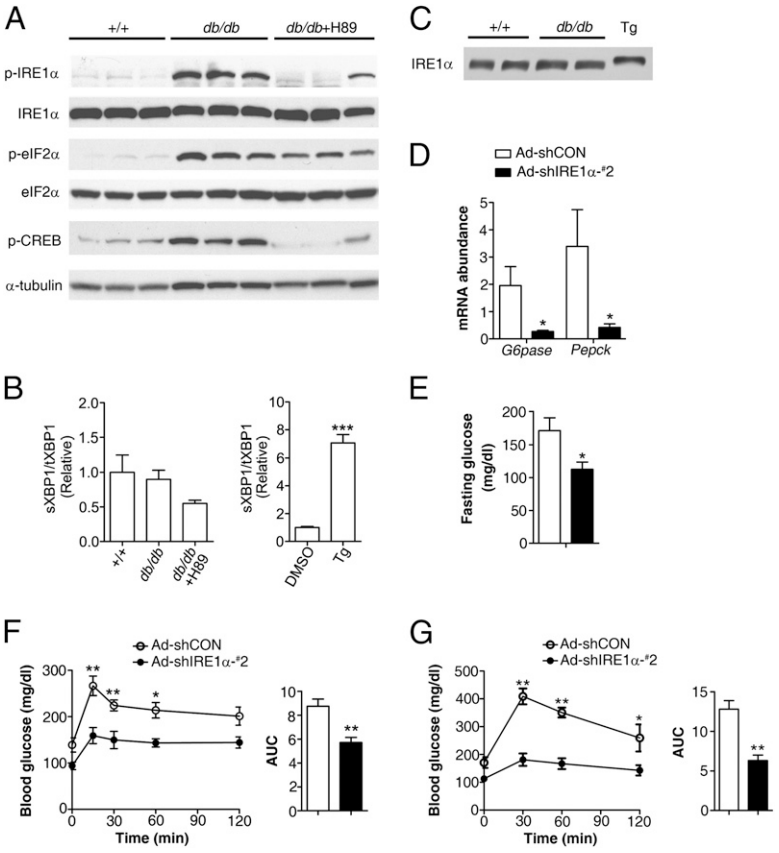

Fig. 5. PKA-dependent hyperactivation of hepatic IRE1α contributes to obesity-associated disruption of glucose metabolism. (*A–C*) Highly increased IRE1α phosphorylation in the livers of *db/db* mice is PKA-dependent and distinct from that induced by ER stress. Male *db/db* mice were treated for 2 h with PBS or H89 (5 mg/kg body weight) through intraperitoneal injection. For ER stress control, primary hepatocytes were treated with 1 μM Tg or DMSO for 1 h. (*A*) Liver extracts from *db/db* mice and their wild-type littermates (+/+) were analyzed by immunoblotting with the indicated antibodies. Shown are representative results for three individual mice from each group (n = 4–5 per group). (*B*) Abundance of the spliced (s) and total (t) *Xbp1* mRNA was determined by real time RT-PCR. (*C*) Band-shift immunoblot analysis of hepatic IRE1α from wild-type or *db/db* mice and from Tg-treated hepatocytes. (*D–G*) Knockdown of hepatic IRE1α improved glucose metabolism in *db/db* mice. Male *db/db* mice were infected with Ad-shCON or Ad-shIRE1α-#2 (n = 5/group). (*D*) At 21 d after infection, the mRNA of liver *G6pase* and *Pepck* was analyzed by real-time RT-PCR after a 6-h fast, using *actin* as an internal control. (*E*) Glucose was measured after a 6-h fast from mice infected for 18 d. (*F* and *G*) Pyruvate tolerance test and glucose tolerance test. Mice infected for 15 or 18 d were fasted for 6 h before intraperitoneal injection with 2 g/kg pyruvate (*F*) or 1.5 g/kg glucose (*G*). Blood glucose was measured at the indicated time points, and the AUCs are shown as the mean ± SEM (n = 5/group). $^*P < 0.05$, $^{**}P < 0.01$ by two-way ANOVA or t test.

type (+/+) littermates, *db/db* animals showed markedly increased phosphorylation of hepatic IRE1α, CREB, and eIF2α (Fig. 5*A*), suggesting simultaneous hyperactivation of PKA and PERK or PKR kinases under obesity-associated metabolic ER stress (20, 33, 34). Surprisingly, this hyperactivation state of IRE1α in *db/db* livers, as detected by prominently elevated Ser^{724} phosphorylation, was not associated with increased *Xbp1* mRNA splicing (Fig. 5*B*); nor did this increased phosphorylation cause a shift of IRE1α protein as that observed upon thapsigargin treatment (Fig. 5*C*). Supporting the idea that increased hepatic PKA activity could largely account for the increased phosphorylation of IRE1α in *db/db* mice, treatment by H89 substantially decreased the phosphorylation of IRE1α as well as CREB but not that of eIF2α (Fig. 5*A* and *SI Appendix*, Fig. S10*B*), accompanied by a considerable reduction of XBP1 splicing. This finding clearly demonstrates that the obesity-associated increase of hepatic IRE1α phosphorylation indeed primarily stemmed from dysregulation of PKA activity (33), rather than from classical ER stress resulting from increased workload of protein folding. Conceivably, in the face of obesity, this PKA-dependent hyperactivation of IRE1α may arise largely from hyperglucagonemia, which plays a critical part in type 2 diabetes (26, 35). Next, we examined whether the highly phosphorylated IRE1α in the liver is an essential contributor to hyperglycemia. Compared with the Ad-shCON–infected control group, adenovirus-mediated knockdown of hepatic IRE1α by Ad-shIRE1α-#2 (*SI Appendix*, Fig. S11*A*) markedly decreased the mRNA abundance of *G6pase* and *Pepck* (Fig. 5*D*), as well as that of the spliced form of XBP1 (*SI Appendix*, Fig. S11*B*), ruling out the involvement of XBP1 in the observed repression of gluconeogenic genes. Moreover, knockdown of hepatic IRE1α expression substantially normalized fasting hyperglycemia in *db/db* mice (Fig. 5*E*) without significantly affecting their body weight (*SI Appendix*, Fig. S11*C*). Additionally, animals with hepatic IRE1α suppression not only exhibited significantly reduced hyperglycemic responses to pyruvate (Fig. 5*F*) or glucagon (*SI Appendix*, Fig. S11*D*), but also showed markedly improved glucose tolerance (Fig. 5*G*). These results further demonstrate that obesity-associated, PKA-dependent hyperactivation enables hepatic IRE1α to act as a critical driver in disrupting glucose homeostasis, suggesting that targeted inhibition of hepatic IRE1α may bear therapeutic benefits against hyperglycemia.

Discussion

Taken together, our findings establish a PKA-dependent mechanism that links the UPR sensor IRE1α to the GPCR signaling pathway in the liver under both physiological and pathophysiological states. As depicted in our proposed model (*SI Appendix*, Fig. S12), upon stimulation by metabolic signals like the GPCR-agonist glucagon, PKA can directly phosphorylate IRE1α at Ser^{724}, a regulatory site that governs its function. This PKA-mediated phosphorylation represents a hitherto unanticipated cytoplasmic event leading to the metabolic activation of IRE1α, which is distinct from that initiated through autophosphorylation in response to the ER luminal events during ER stress (i.e., accumulation of unfolded/misfolded proteins). Metabolic activation by the glucagon pathway of hepatic IRE1α can exert a range of metabolic effects, including regulation of the gluconeogenic program in an XBP1-independent manner.

Currently, it remains an open question how IRE1α, upon phosphorylation by PKA from the cytoplasm, can exert its effect on glucagon-regulated metabolic programs in the liver. Because we observed a lack of involvement of XBP1 splicing in IRE1α-dependent up-regulation of gluconeogenic genes, it is possible that the acute activation mode of IRE1α evoked by the glucagon-PKA pathway may be separated from activation of its XBP1-specific RNase activity. On the other hand, under conditions of chronic glucagon exposure, it is unclear whether PKA-dependent IRE1α phosphorylation can promote the activation of its RNase activity for XBP1 splicing, and the precise metabolic action of the endogenous sXBP1 in this setting also remains elusive. However, given the multitude of downstream signaling events that can be engaged following IRE1α activation (36), it is not

unreasonable to speculate that RNase-independent mechanisms may exist to execute its metabolic actions in response to glucagon stimulation.

It is interesting to note that another UPR sensor ATF6, upon activation by classic ER stress, was reported to interact with CRTC2 and disturb its ability to coactivate CREB for up-regulating gluconeogenic genes (16). In addition, hepatic overexpression of the sXBP1 protein, the molecule targeted by IRE1α during typical ER stress, was shown to repress the expression of gluconeogenic genes and improve glucose metabolism in the insulin resistant *ob*/*ob* mice (31). Whereas a recent study showed that alterations of lipid composition in the ER contributed to increased phosphorylation of IRE1α in the obese livers (37), our results apparently unmasked a distinct PKA-dependent activation mode of IRE1α that acted, without involving the splicing of *Xbp1* mRNA, as a critical driver of hyperglycemia in *db*/*db* mice. Thus, it seems that dysregulated metabolic signals leading to an increase in the PKA activity in the cytoplasm, as well as aberrant lipid and calcium metabolism in the ER, are both responsible for the metabolic hyperactivation of IRE1α under obesity-associated ER stress conditions. Nonetheless, given the broad roles of the GPCR-PKA pathway in a myriad of biological processes, modulation of the IRE1α pathway in this context may offer valuable therapeutic leads against many human diseases including diabetes.

Materials and Methods

Animal Studies. Male wild-type C57BL/6J mice were purchased from Shanghai Laboratory Animal Co. Ltd., and male C57BL/6J *db/db* mice and their wild-type littermates were from Model Animal Research Center, Nanjing University. Animals were housed in laboratory cages at a temperature of 23 ± 3 °C and a humidity of 35 ± 5% under a 12-h dark/light cycle with free access to standard chow (Shanghai Laboratory Animals Co.) and water in accredited animal facilities. All animals were killed under anesthetic conditions or by cervical dislocation. Livers were snap-frozen in liquid nitrogen immediately after resection and stored at −80 °C. All experimental protocols were approved by the Institutional Animal Care and Use Committee at the Institute for Nutritional Sciences, Shanghai Institutes for Biological Sciences, Chinese Academy of Sciences. Adenovirus administration, glucagon challenge test, and glucose or pyruvate tolerance test were carried out as described in the *SI Appendix, Materials and Methods*.

Isolation of Primary Hepatocytes and Adenovirus Infection. Primary hepatocytes were isolated from male C57BL/6J mice at 8 to 12 wk of age. Hepatocytes were infected for 48 or 72 h with adenoviruses at a multiplicity of infection of 40 and were treated with the desired reagents before protein extraction for Western immunoblot analysis. Generation of recombinant adenoviruses was as described in the *SI Appendix, Materials and Methods*.

Detailed materials and experimental procedures for immunoblotting, RT-PCR, IRE1α phosphorylation analyses, glucose production assays, and microarray analyses were all described in *SI Appendix, Materials and Methods*.

Statistical Analysis. All data are presented as the mean ± SEM. Statistical analysis was performed using unpaired two-tailed *t* test, and one-way or two-way ANOVA followed by Bonferroni's post test with GraphPad Prism 5.0. $P < 0.05$ was considered to be statistically significant.

ACKNOWLEDGMENTS. We thank Hua-sheng Xiao and Li Zhu for conducting microarray assays, Shan-shan Pang for assisting with tail-vein adenoviral injection, and Zheng-Gang Liu and Charles E. Samuel for critical reading of the manuscript. This work was supported by Grants 81021002, 30988002, 90713027, 30830033, and 30970584 from the National Natural Science Foundation, the Ministry of Science and Technology (973 Program 2011CB910900 and 2007CB947100), the Chinese Academy of Sciences (Knowledge Innovation Programs KSCX2-EW-R-09 and KSCX1-YW-02; Chief Scientist Program-SIBS2008006; and the Chinese Academy of Sciences/State Administration of Foreign Experts Affairs International Partnership Program); Science and Technology Commission of Shanghai Municipality Grants 10XD1406400 and 08dj1400601 (to Yong Liu and W.L.); and Ministry of Science and Technology Grant 2006BAI23B00 (to X.G.).

1. Ron D, Walter P (2007) Signal integration in the endoplasmic reticulum unfolded protein response. *Nat Rev Mol Cell Biol* 8:519–529.
2. Patil C, Walter P (2001) Intracellular signaling from the endoplasmic reticulum to the nucleus: The unfolded protein response in yeast and mammals. *Curr Opin Cell Biol* 13: 349–355.
3. Mori K, Ma W, Gething MJ, Sambrook J (1993) A transmembrane protein with a cdc2+/CDC28-related kinase activity is required for signaling from the ER to the nucleus. *Cell* 74:743–756.
4. Sidrauski C, Walter P (1997) The transmembrane kinase Ire1p is a site-specific endonuclease that initiates mRNA splicing in the unfolded protein response. *Cell* 90: 1031–1039.
5. Cox JS, Shamu CE, Walter P (1993) Transcriptional induction of genes encoding endoplasmic reticulum resident proteins requires a transmembrane protein kinase. *Cell* 73:1197–1206.
6. Shamu CE, Walter P (1996) Oligomerization and phosphorylation of the Ire1p kinase during intracellular signaling from the endoplasmic reticulum to the nucleus. *EMBO J* 15:3028–3039.
7. Welihinda AA, Kaufman RJ (1996) The unfolded protein response pathway in *Saccharomyces cerevisiae*. Oligomerization and trans-phosphorylation of Ire1p (Ern1p) are required for kinase activation. *J Biol Chem* 271:18181–18187.
8. Calfon M, et al. (2002) IRE1 couples endoplasmic reticulum load to secretory capacity by processing the XBP-1 mRNA. *Nature* 415:92–96.
9. Lee K, et al. (2002) IRE1-mediated unconventional mRNA splicing and S2P-mediated ATF6 cleavage merge to regulate XBP1 in signaling the unfolded protein response. *Genes Dev* 16:452–466.
10. Yoshida H, Matsui T, Yamamoto A, Okada T, Mori K (2001) XBP1 mRNA is induced by ATF6 and spliced by IRE1 in response to ER stress to produce a highly active transcription factor. *Cell* 107:881–891.
11. Han D, et al. (2009) IRE1alpha kinase activation modes control alternate endoribonuclease outputs to determine divergent cell fates. *Cell* 138:562–575.
12. Ali MM, et al. (2011) Structure of the Ire1 autophosphorylation complex and implications for the unfolded protein response. *EMBO J* 30:894–905.
13. Lee KP, et al. (2008) Structure of the dual enzyme Ire1 reveals the basis for catalysis and regulation in nonconventional RNA splicing. *Cell* 132:89–100.
14. Korennykh AV, et al. (2009) The unfolded protein response signals through high-order assembly of Ire1. *Nature* 457:687–693.
15. Hotamisligil GS (2010) Endoplasmic reticulum stress and the inflammatory basis of metabolic disease. *Cell* 140:900–917.
16. Wang Y, Vera L, Fischer WH, Montminy M (2009) The CREB coactivator CRTC2 links hepatic ER stress and fasting gluconeogenesis. *Nature* 460:534–537.
17. Lipson KL, et al. (2006) Regulation of insulin biosynthesis in pancreatic beta cells by an endoplasmic reticulum-resident protein kinase IRE1. *Cell Metab* 4:245–254.
18. Qiu Y, et al. (2010) A crucial role for RACK1 in the regulation of glucose-stimulated IRE1alpha activation in pancreatic beta cells. *Sci Signal* 3:ra7.
19. Yusta B, et al. (2006) GLP-1 receptor activation improves beta cell function and survival following induction of endoplasmic reticulum stress. *Cell Metab* 4:391–406.
20. Eizirik DL, Cardozo AK, Cnop M (2008) The role for endoplasmic reticulum stress in diabetes mellitus. *Endocr Rev* 29:42–61.
21. Ozcan U, et al. (2006) Chemical chaperones reduce ER stress and restore glucose homeostasis in a mouse model of type 2 diabetes. *Science* 313:1137–1140.
22. Ozcan L, et al. (2009) Endoplasmic reticulum stress plays a central role in development of leptin resistance. *Cell Metab* 9:35–51.
23. Zhang X, et al. (2008) Hypothalamic IKKbeta/NF-kappaB and ER stress link overnutrition to energy imbalance and obesity. *Cell* 135:61–73.
24. Zhang K, et al. (2011) The unfolded protein response transducer IRE1α prevents ER stress-induced hepatic steatosis. *EMBO J* 30:1357–1375.
25. Ritter SL, Hall RA (2009) Fine-tuning of GPCR activity by receptor-interacting proteins. *Nat Rev Mol Cell Biol* 10:819–830.
26. Jiang G, Zhang BB (2003) Glucagon and regulation of glucose metabolism. *Am J Physiol Endocrinol Metab* 284:E671–E678.
27. Murray AJ (2008) Pharmacological PKA inhibition: All may not be what it seems. *Sci Signal* 1:re4.
28. Kennelly PJ, Krebs EG (1991) Consensus sequences as substrate specificity determinants for protein kinases and protein phosphatases. *J Biol Chem* 266:15555–15558.
29. Lee AH, Scapa EF, Cohen DE, Glimcher LH (2008) Regulation of hepatic lipogenesis by the transcription factor XBP1. *Science* 320:1492–1496.
30. Rutkowski DT, et al. (2008) UPR pathways combine to prevent hepatic steatosis caused by ER stress-mediated suppression of transcriptional master regulators. *Dev Cell* 15:829–840.
31. Zhou Y, et al. (2011) Regulation of glucose homeostasis through a XBP-1-FoxO1 interaction. *Nat Med* 17:356–365.
32. Cunha DA, et al. (2009) Glucagon-like peptide-1 agonists protect pancreatic beta-cells from lipotoxic endoplasmic reticulum stress through upregulation of BiP and JunB. *Diabetes* 58:2851–2862.
33. Erion DM, et al. (2009) Prevention of hepatic steatosis and hepatic insulin resistance by knockdown of cAMP response element-binding protein. *Cell Metab* 10:499–506.
34. Nakamura T, et al. (2010) Double-stranded RNA-dependent protein kinase links pathogen sensing with stress and metabolic homeostasis. *Cell* 140:338–348.
35. Gelling RW, et al. (2003) Lower blood glucose, hyperglucagonemia, and pancreatic alpha cell hyperplasia in glucagon receptor knockout mice. *Proc Natl Acad Sci USA* 100:1438–1443.
36. Hetz C, Glimcher LH (2009) Fine-tuning of the unfolded protein response: Assembling the IRE1alpha interactome. *Mol Cell* 35:551–561.
37. Fu S, et al. (2011) Aberrant lipid metabolism disrupts calcium homeostasis causing liver endoplasmic reticulum stress in obesity. *Nature* 473:528–531.